THE JOURNAL OF BIOLOGICAL CHEMISTRY VOL. 283, NO. 52, pp. 36624–36635, December 26, 2008

ABCA12 Maintains the Epidermal Lipid Permeability Barrier by Facilitating Formation of Ceramide Linoleic Esters*[S]

Received for publication, September 24, 2008, and in revised form, October 26, 2008 Published, JBC Papers in Press, October 27, 2008, DOI 10.1074/jbc.M807377200

Ying Zuo[‡§], Debbie Z. Zhuang[‡§], Rong Han[¶], Giorgis Isaac[‖], Jennifer J. Tobin[‡§], Mary McKee[**], Ruth Welti[‖], Janice L. Brissette[¶], Michael L. Fitzgerald[‡§], and Mason W. Freeman[‡§1]

From the [‡]Lipid Metabolism Unit and Department of Medicine, the [§]Center for Computational & Integrative Biology, the [¶]Cutaneous Biology Research Center, and the [**]Center for Membrane Biology, Massachusetts General Hospital and Harvard Medical School, Boston, Massachusetts 02114 and the [‖]Division of Biology, Kansas State University, Manhattan, Kansas 66506

Harlequin ichthyosis is a congenital scaling syndrome of the skin in which affected infants have epidermal hyperkeratosis and a defective permeability barrier. Mutations in the gene encoding a member of the ABCA transporter family, ABCA12, have been linked to harlequin ichthyosis, but the molecular function of the protein is unknown. To investigate the activity of ABCA12, we generated *Abca12* null mice and analyzed the impact on skin function and lipid content. *Abca12*$^{-/-}$ mice are born with a thickened epidermis and die shortly after birth, as water rapidly evaporates from their skin. *In vivo* skin proliferation measurements suggest a lack of desquamation of the skin cells, rather than enhanced proliferation of basal layer keratinocytes, accounts for the 5-fold thickening of the *Abca12*$^{-/-}$ stratum corneum. Electron microscopy revealed a loss of the lamellar permeability barrier in *Abca12*$^{-/-}$ skin. This was associated with a profound reduction in skin linoleic esters of long-chain ω-hydroxyceramides and a corresponding increase in their glucosyl ceramide precursors. Because ω-hydroxyceramides are required for the barrier function of the skin, these results establish that ABCA12 activity is required for the generation of long-chain ceramide esters that are essential for the development of normal skin structure and function.

Harlequin ichthyosis (HI)[2] is the most severe of the congenital, autosomal ichthyoses with affected infants developing large, hard, plate-like scales over all of their epidermal surfaces. Abnormal temperature regulation, enhanced water loss, and bacterial super-infections develop as a consequence of defects in the barrier functions of the skin, making survival through the neonatal period difficult. In recent years, several groups have linked HI, as well as less severe forms of ichthyosis, to mutations in the gene encoding a member of the ABCA family of transporters, ABCA12 (1–7). The A class of ABC transporters consists of at least eleven transporters in humans and mice, several of which are known to play critical roles in human disease. ABCA1, the best studied of the proteins, is causally linked to Tangier disease and is associated with defective phospholipid and cholesterol transport from intracellular lipid stores to the major amphipathic helical apoprotein of high density lipoprotein, apolipoprotein A-1 (8–11). ABCA3 mutations cause a form of neonatal respiratory failure that arises from a failure to transport pulmonary phospholipids comprising surfactant from their storage site in the lamellar bodies of alveolar type II cells to the alveolar space (12–14). This transport process, like the one involving ABCA1, appears to depend on the lipidation of an acceptor amphipathic helical protein, surfactant protein B (15, 16). ABCA4 causes Stargadt macular degeneration and visual loss that is associated with a defect in the transport of phosphatidylethanolamine-retinylidene adducts out of retinal pigment epithelial cells (17–19). The role of any acceptor proteins in this process is unknown. The transport activities of the other members of the ABCA proteins remain to be clarified, but the molecular precedents noted above strongly suggested that ABCA12 would also play a role in lipid transport. In fact, initial studies of the skin of individuals affected with HI strengthened this hypothesis when it was observed that keratinocytes within the granular layer of HI skin contained abnormal lamellar granules and malformed intercellular lipid layers in the stratum corneum (20, 21).

As part of a general effort to elucidate mechanisms of lipid transport by members of the ABCA family, we have initiated a program to inactivate these transporters using homologous recombinant methodologies in the mouse (16, 22). In this report, we present data on mice lacking functional ABCA12. These mice provide a remarkable model of human HI in that

* This work was supported, in whole or in part, by National Institutes of Health Grants RR020345 (to M. W. F.) and HL074136 (to M. L. F.). The electron microscopy core is supported by an Inflammatory Bowel Disease Grant (DK43351) and a Boston Area Diabetes and Endocrinology Research Center Award (DK57521). The Kansas Lipidomics Research Center (KLRC) was supported by National Science Foundation (NSF) Grants MCB 0455318 and DBI 0521587, and NSF EPSCoR Grant EPS-0236913, with matching support from the State of Kansas through Kansas Technology Enterprise Corporation and Kansas State University. The KLRC was also supported by Kansas Idea Network of Biomedical Research Excellence from NIH Grant P20 RR16475, from the Idea Network of Biomedical Research Excellence program of the National Center for Research Resources. The costs of publication of this article were defrayed in part by the payment of page charges. This article must therefore be hereby marked "*advertisement*" in accordance with 18 U.S.C. Section 1734 solely to indicate this fact.

[S] The on-line version of this article (available at http://www.jbc.org) contains supplemental Figs. S1–S10.

[1] To whom correspondence should be addressed: Dept. of Medicine and Center for Computational & Integrative Biology, Simches 7214, Massachusetts General Hospital, 185 Cambridge St., Boston, MA 02114. Tel.: 617-726-5906; Fax: 617-726-2879; E-mail: freeman@molbio.mgh.harvard.edu.

[2] The abbreviations used are: HI, harlequin ichthyosis; ABCA12, ATP cassette binding transporter A12; BrdUrd, bromodeoxyuridine; Cer, ceramide; Cer(EOS), linoleic ester of ω-hydroxyceramides; GlcCer(EOS), glucosyl precursor of Cer(EOS); Cer(OS), non-esterified hydroxyceramides; Cer(NS), non-hydroxyceramides; ESI, electrospray ionization; TEWL, trans-epidermal water loss; PBS, phosphate-buffered saline; MS, mass spectrometry.

they develop a markedly thickened stratum corneum and defects in the skin lipid barrier, as evidenced by electron microscopy and functional assays of tissue water loss. To better characterize the lipid barrier defect, an extensive analysis of the lipid content of the skin of the ABCA12-deficient mice was performed. As ceramides are the major lipid constituent of lamellar sheets in the intercellular spaces of the stratum corneum, attention was particularly focused on this class of lipids. Using mass spectrometry, we were able to establish that a marked decrease in multiple species of Ceramide 1 (also called Cer(EOS) or esterified ω-hydroxy acid sphingosine) was present in *Abca12* null mice. This was associated with a significant increase in the amount of precursor EOS-glucosyl ceramide in the skin, suggesting that a loss of ABCA12 activity leads to a failure to transport glucosylceramides to a location where cleavage of the sugar moiety by glucocerebrosidase can occur. These findings indicate that *Abca12* null mice are an excellent model of human harlequin ichthyosis, and they demonstrate that ABCA12 activity is required for the generation of a specific class of lipids that are essential to the formation of the epidermal permeability barrier.

EXPERIMENTAL PROCEDURES

Generation and Genotyping of Abca12 Null Mice—Mice that were heterozygous for recombination at the Abca12 locus were obtained through the National Institutes of Health Mutant Mouse Resource Center, University of California, Davis. These mice were generated by replacing exon 9 of Abca12 with a Neo^R cassette via homologous recombination. To confirm the genotype of these mice, Southern hybridization was conducted using genomic DNA cleaved with the SpeI restriction endonuclease and a radiolabeled cDNA fragment that hybridizes to intron 7/8 (nucleotides 4440–5010) of the Abca12 locus. This probe detects a band of 15.4 kb in the wild-type locus and 8 kb in the targeted gene. For PCR genotyping, three primer multiplex reactions were used (P1, common, 5′-GGGGCGGTGAGAAGTAAAGTAT-3′; P2, wild-type allele, 5′-GGATTGGGAAGACAATAGCAGG-3′; P3, targeted allele, 5′-CTTGGCAGAGTACATCTCAG-3′) that amplify a wild-type product of 356 bp and a targeted product of 271 bp. F2 heterozygous animals (129SvEvBrd × C57BL6/J) were intercrossed to produce homozygous $Abca12^{-/-}$ mice, as well as wild-type and heterozygous littermates. All animal procedures were approved by the Massachusetts General Hospital Subcommittee on Research Animal Care and were conducted in accordance with the USDA Animal Welfare Act and the PHS Policy for the Humane Care and Use of Laboratory Animals.

ABCA12 mRNA Quantitation—Total RNA was extracted using the RNeasy Mini Kit (Qiagen) according to the manufacturer's instructions (Qiagen). RNA concentration and quality were assessed using the Agilent RNA Bioanalyzer. RNA (1 μg) was reversed transcribed using the SuperScript First-Strand Synthesis System for RT-PCR (Invitrogen), and quantitative real-time PCR reactions were performed on a Thermal cycler (Thermo Fisher Scientific, Waltham, MA). Levels of β-actin mRNA were used to normalize ABCA12 mRNA levels. The primer pairs were as follows: ABCA12, 5′-AAGATGCTGACTGGAGACATAATTC-3′ and 5′-GAAATACAAGTGCTCTTCCACAGTT-3′, which amplify exons 46 and 47 of the Abca12 mRNA, and 5′-CATACAAGCCACTGTTATCCTCC-3′ and 5′-CAGAGATTTCGTACCTCTCCTCA-3′, which amplify the β-actin mRNA.

In Situ Hybridization—Automated *in situ* hybridization was performed using the Discovery System (Ventana Medical Systems, Tucson, AZ). Sense and antisense probes that hybridize to exons 46–51 of the *Abca12* mRNA were generated using digoxigenin-labeled UTP. The efficiency of transcription and incorporation of digoxigenin-UTP to the riboprobes were evaluated by 5% acrylamide-urea gel electrophoresis and dot blot on nylon membrane, respectively (DIG Nucleic Acid Detection Kit, nitro blue tetrazolium/5-bromo-4-chloro-3-indolyl phosphate, Roche Molecular Biochemicals, Mannheim, Germany). Slides were hybridized at 65 °C for 6 h, washed twice in 0.1× SSC buffer at 75 °C, each for 6 min. The detection was performed using biotinylated anti-digoxigenin antibody (Biogenex, San Ramon, CA) followed by streptavidin-alkaline-phosphatase conjugate and visualized by nitro blue tetrazolium/5-bromo-4-chloro-3-indolyl phosphate substrate reaction (Ventana BlueMap Detection Kit, Ventana Medical Systems, Tucson, AZ). Slides were counterstained by nuclear fast red (Vector Laboratories, Inc., Burlingame, CA).

Immunoblotting Procedures and Generation of an ABCA12 Antibody—Mouse ABCA12 cDNA was amplified by RT-PCR from adult C57/BL6 skin total RNA, and the sequence was verified on both strands by dideoxy sequencing. An anti-ABCA12 anti-serum was raised against the C-terminal 98 amino acids of murine ABCA12 as we previously described for ABCA1 (23). The specificity of the sera obtained was confirmed by immunoblotting of lysates from HEK293 cells transfected with the cDNAs of ABCA12, ABCA7, or ABCA1, using the ABCA12 antiserum (diluted 1:1000) and pre-immune control serum (diluted 1:1000). The antiserum recognized a band of ~290 kDa only in lysates of cells transfected with the ABCA12 cDNA. Equal amounts of skin lysates (20 μg of total cell protein in a lysis buffer composed of 20 mM Tris-HCl, pH 7.5, 150 mm NaCl, 1 mM EDTA, 1% Nonidet P-40, 0.5% deoxycholate, 0.1% SDS, and 0.001% Sigma protease mixture) were electrophoresed on 4–12% or 6% SDS-PAGE gels and transferred onto nitrocellulose membranes. Membranes were blocked overnight at 4 °C in 1× PBS, 5% nonfat dry milk, and 1% bovine serum albumin, and were probed with the anti-ABCA12 or anti-ABCA1 antiserum, diluted 1:1000, at room temperature for 2 h. Membranes were washed in 1× PBS containing 0.1% Tween 20. Antibody binding was detected using a horseradish peroxidase-conjugated goat anti-rabbit antibody (Sigma) and enhanced chemiluminescence (Amersham Biosciences). For analysis of filaggrin solubility and processing, skin lysates were prepared with the buffer as above, or with a denaturing thiocyanate buffer (1 M NaSCn, 50 mM HEPES, 10 mM EDTA, 0.3 mM *ortho*-phenanthroline, 20 μg/ml phenylmethylsulfonyl fluoride, and 0.1% isopropanol) as previously described (24, 25). To enhance extraction of cornified proteins using the thiocyanate buffer, lysates were sonicated and snap frozen (2×). Precipitated proteins were solubilized in 8 M urea before boiling in reducing SDS loading buffer.

Histological, Immunofluorescent, and Ultrastructural Procedures—For hematoxylin and eosin (H&E) histological analysis, skin samples were fixed overnight (4% formaldehyde, 1× PBS, 4 °C), embedded in paraffin, and 5-μm sections were stained and imaged using a Nikon Eclipses 50i microscope. For immunofluorescence staining, OCT-embedded skin was snap frozen in liquid nitrogen-cooled isopentane, and sections (5 μm) were fixed (acetone:methanol (1:1), −20 °C) and blocked with Superblock (Thermo Scientific) (26). Slides were incubated with primary antibodies for loricrin, filaggrin, K10, K14 (Covance), and Ki67b (Abcam Inc.), or with an equivalent amount of non-immune rabbit IgG. They were washed three times (0.1% Nonidet P-40, 1× PBS) and primary antibody binding was detected with a CY3-labeled goat anti-rabbit IgG antibody (Santa Cruz Biotechnology, Santa Cruz, CA). Nuclei were counterstained with Hoechst 33258 dye (1 μg/ml, 0.1% Nonidet P-40, 1× PBS) (Sigma-Aldrich), and slides were imaged using a Nikon OPTIPHOT photomicroscope (Nikon Eclipse E 800).

For electron microscopy studies, skin taken from littermate E18.5 embryos was prepared and imaged as described previously (27). In brief, dorsal skin was fixed overnight at 4 °C in 2% glutaraldehyde, 2% paraformaldehyde, with 0.06% calcium chloride in 0.1 M sodium cacodylate buffer (pH 7.3). Skin samples were post-fixed (0.2% ruthenium tetroxide, 0.5% potassium ferrocyanide in 0.1 M sodium cacodylate, pH 6.8, room temp in darkness, 30 min), dehydrated, and embedded in Eponˆ812 resin (Electron Microscopy Sciences, Hatfield, PA). Ultrathin sections cut on a Reichert Ultracut E ultramicrotome were collected onto Formvar-coated slot grids and examined unstained or after double staining with uranyl acetate and lead citrate using a JEOL 1011 transmission electron microscope with an ATM digital camera at 80 kV. A survey of corneocyte interstitial lamellae and granulocyte lamellar storage bodies in the epidermis of littermate-paired E18.5 pups ($Abca12^{+/+}$ and $Abca12^{-/-}$; $n = 3$) was carried out on 100 micrographs at magnifications of 80,000–120,000.

In Utero BrdUrd Incorporation and Imaging—Pregnant mice were injected intraperitoneally with 5-bromo-2′-deoxyuridine (BrdUrd, 100 μg/g, Invitrogen) and sacrificed 1 h later as described with the following modifications (28). Dorsal skin from the labeled E18.5 embryos was embedded, sectioned, and fixed as described above, and slides were stained with an anti-BrdU antibody (Invitrogen). Nuclei were counterstained with Hoechst 33258 dye (Sigma-Aldrich). IP Lab Spectrum software (4.0) was used to quantify the area of BrdUrd-positive nuclei per area of epidermal tissue (Scanalytics, Rockville, MD). Average values derived from five images of each embryo sample were compared ($Abca12^{+/+}$, $n = 3$ and $Abca12^{-/-}$, $n = 4$).

Skin Permeability Assays—Dye penetration assays were performed with toluidine blue as previously described (29). In brief, E18.5 embryos were dehydrated by incubations in 25%, 50%, 75%, and 100% methanol/PBS (1 min per incubation). The embryos were washed in PBS and stained in 0.0125% toluidine blue for 10 min. After staining, embryos were immediately washed in PBS three times and photographed. Trans epidermal water loss (TEWL) was measured in 1-cm^2 skin sections using a gravimetric assay as previously described (30).

Mass Spectrometry Lipid-profiling Procedures—Phospholipids in skin lysates from individual E18.5 embryos were determined using an electrospray ionization-MS/MS approach as reported previously (16). In brief, skin (~5–10 mg) cleaned of all subcutaneous tissue ($Abca12^{+/+}$ and $Abca12^{-/-}$ E18.5 embryos, $n = 5$) was minced with scissors and vortex-homogenized with steel beads in 0.5 ml of 1× PBS (BioSpec, Bartlesville, OK). Homogenate was extracted with 2.5 ml of chloroform/methanol/distilled water (1:1:0.5, v/v), and two 0.5-ml chloroform extractions. Combined organic phases were wash with 0.5 ml of KCl (1 M, 1×) and with 0.5 ml of dH_20 (2×) and dried with N_2 gas. Samples were resuspended in 1 ml of chloroform, and phospholipid scans were performed as described (16). To analyze ceramides and glucosylceramides, additional scans were performed for precursors of m/z 264 in the positive mode (collision energy, 50 V) for GlcCers and high mass Cers and neutral loss of m/z 316 in the negative mode (collision energy, 50 V) for low mass Cers. Internal standards for quantitating these sphingolipids were d18:1/14:0Cer and d18:1/12:0GalCer.

Levels of free fatty acids in skin lysates from individual E18.5 embryos were determined by methyl esterification (22): samples were mixed with methanol:methylene chloride and acetyl chloride, incubated for 1 h at 75 °C, cooled, and then 7% potassium carbonate was added. Lipids were extracted with hexane, washed with acetonitrile and injected (splitless) into an Agilent 6890 gas chromatography-MS (G2613A system, Agilent Technologies, Palo Alto, CA) equipped with a Supelcowax-10 column (30 m × 0.25 mm × 0.25 μm film, Supelco, Bellafonte, PA). The temperature program for the gas chromatography oven was as follows: Initial temperature 150 °C for 2 min, increased to 200 °C (10 °C/min), held at 200 °C for 4 min, increased to 240 °C (5 °C/min), held at 240 °C for 3 min, and finally increased to 270 °C (10 °C/min) and held at 270 °C for 5 min. A model 5973N mass-selective detector (Agilent Technologies) in scan mode and coupled with Enhanced Chemstation G1701CA version C software was used to identify the generated mass spectra by comparison to a spectral library created from known fatty acids. The amount of each fatty acid species was quantified relative to an internal standard of heptadecanoic acid (17:0) added to the samples before extraction. Total cholesterol in the skin was determined as previously described (31).

Statistical Analysis—All statistical analyses were performed using Student's t test with sample sizes indicated in the figure legends for each comparison that was made. A p value of <0.05 was considered statistically significant.

RESULTS

Homozygous Null $Abca12^{-/-}$ Mutations in Mice Result in Neonatal Lethality and Epidermal Hyperkeratosis—The targeting strategy used to produce mice lacking ABCA12 is shown in Fig. 1*A*. To confirm that the heterozygous mice we obtained from the NIH Mutant Mouse Resource had the correctly rearranged gene structure, we performed Southern blot analysis. Appropriate homologous recombination leading to the deletion of exon 9 was confirmed in E18.5 embryos derived from $Abca12^{+/-}$ heterozygous matings (Fig. 1*B*). One or both wild-type 15.4-kb SpeI fragments were replaced by an 8.0-kb band in

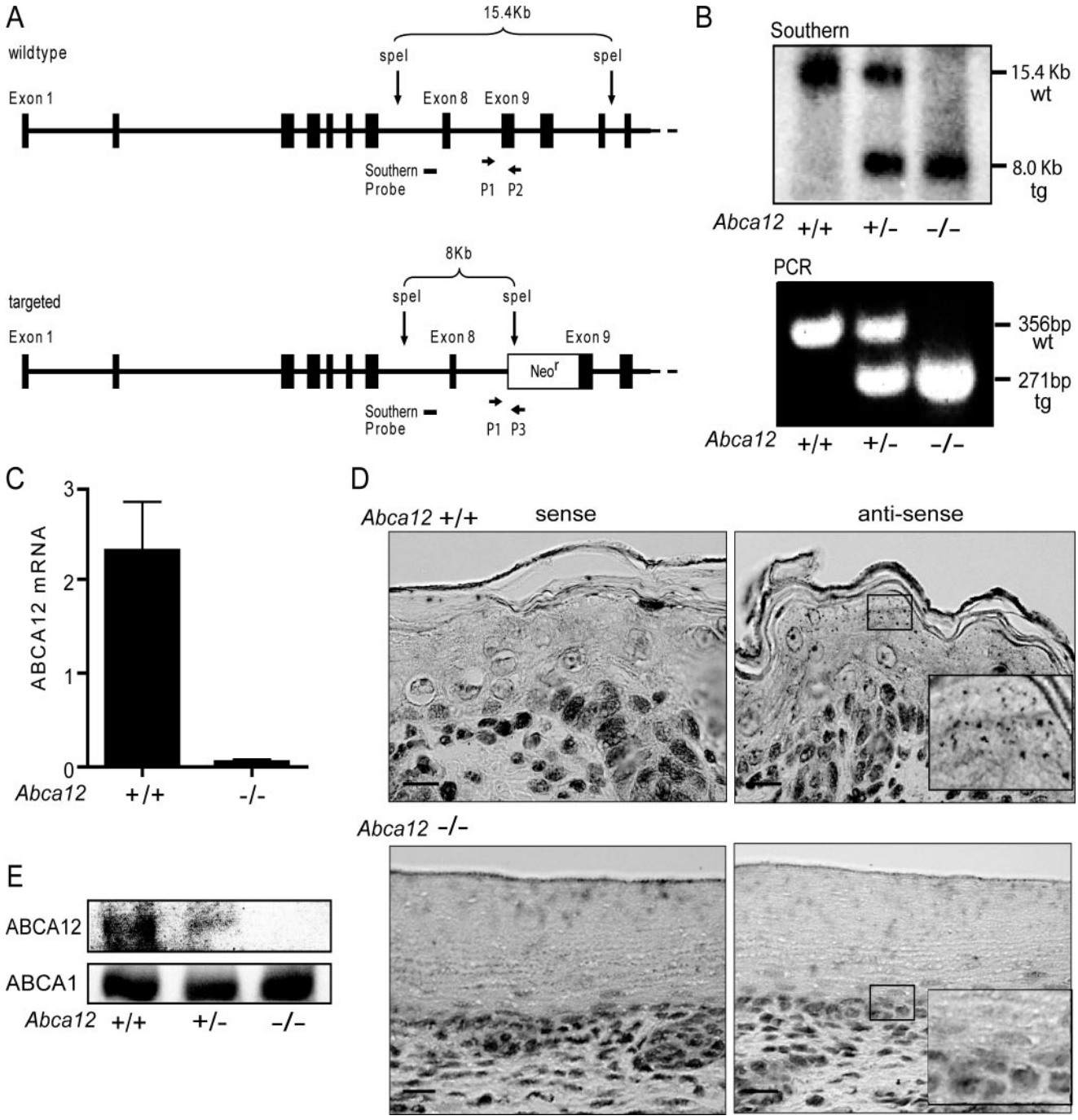

FIGURE 1. **Deletion of Abca12 exon 9 in mice blocks ABCA12 expression.** *A*, exon 9 of the Abca12 locus (*wt*) was disrupted by homologous recombination. The resulting targeted allele (*tg*) contains a NeoR cassette and truncates the 2596-amino acid ABCA12 open reading frame after amino acid 328. *B*, Southern and PCR analysis of DNA from day 18.5 embryos demonstrated transmission of the targeted allele and generation of the null state. Position of the DNA probe and PCR primers are indicated in the *diagram*. ABCA12 mRNA levels are significantly diminished in the *Abca12*$^{-/-}$ mice as determined by quantitative RT-PCR ($n = 5$, $\pm$S.D., $p < 0.5$) (*C*) and by *in situ* hybridization (*D*); *scale bar*, 20 μm. *E*, *Abca12*$^{-/-}$ mice lack ABCA12 protein as determined by immunoblots of skin lysates using anti-ABCA12 C-terminal antibody. Serial probing of the blot for ABCA1, an ABCA12 homologue, demonstrated equal loading of the membrane, and no compensatory change in ABCA1 expression.

animals heterozygous or homozygous, respectively, for the targeted gene locus. Having established by Southern blot that the desired homologous recombination at exon 9 of the Abca12 locus had occurred in parental strains, high throughput genotyping of mouse offspring was subsequently performed using an assay that enabled all three potential genotypes to be determined in a single, multiplexed PCR reaction (Fig. 1*B*). To establish that the gene rearrangement led to loss of expression of ABCA12, assays of both ABCA12 mRNA and protein levels were performed. ABCA12 message levels in the skin were first determined using reverse transcriptase-quantitative PCR amplifications of exons (46 and 47) downstream of the deleted exon 9. Fig. 1*C* demonstrates that, although wild-type animals have readily detected levels of ABCA12 mRNA, null mice do not. These data indicate that the targeted deletion of exon 9 results in the production of an mRNA that is either unstable or

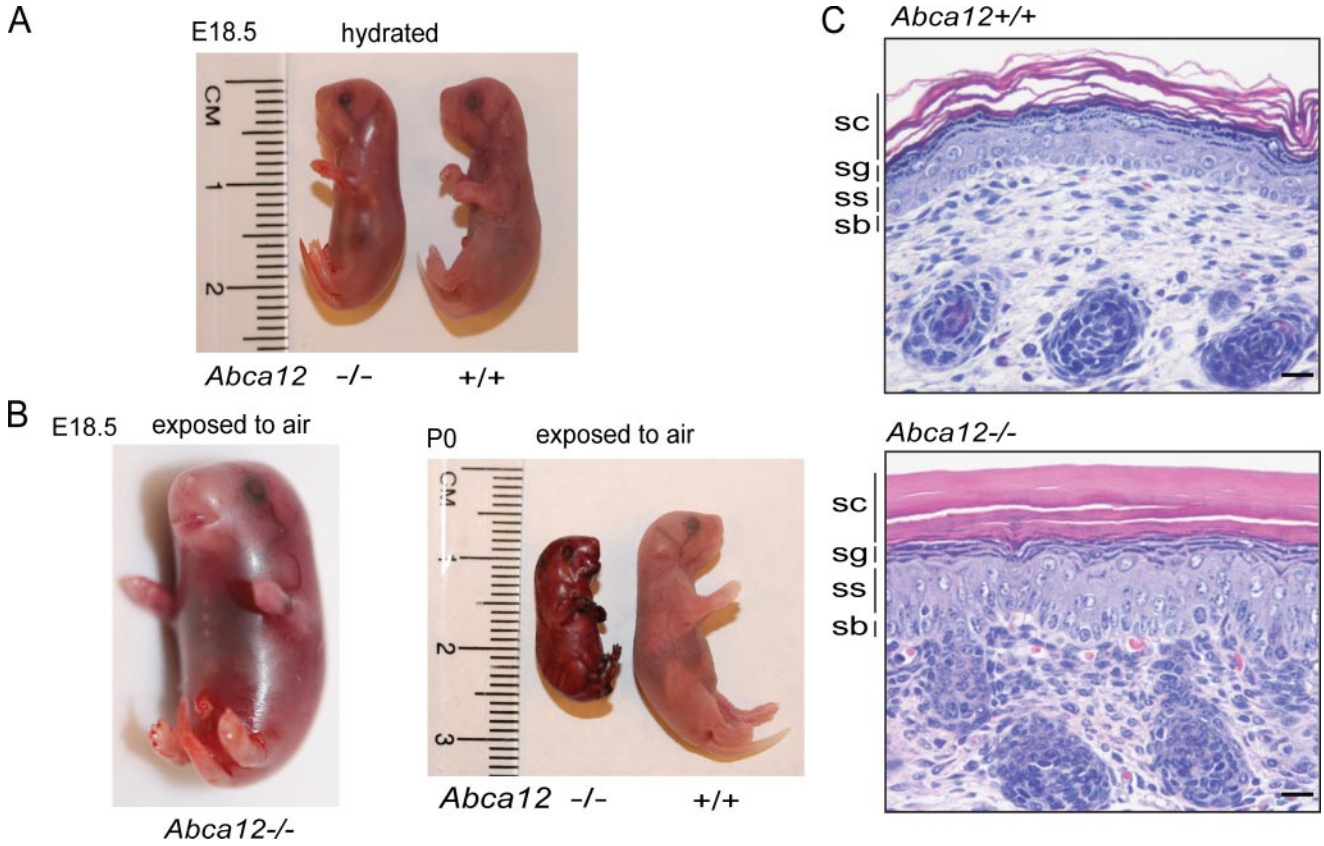

FIGURE 2. **Loss of ABCA12 cause neonatal lethality and epidermal hyperkeratosis.** *A*, *Abca12*$^{-/-}$ day 18.5 embryos (E18.5) when kept hydrated are similar in size and weight to *Abca12*$^{+/+}$ littermates, but after exposure to air rapidly dry out and become encased in a collodion-like shell (*B*). The *Abca12*$^{-/-}$ epidermis displays a markedly thickened, hyperkeratotic epidermis as shown in hematoxylin & eosin-stained skin sections; *scale bar*, 20 μm (*C*) (*sc* = stratum corneum, *sg* = stratum granulosum, *ss* = stratum spinosum, and *sb* = stratum basale).

poorly transcribed. These *in vitro* amplification results were confirmed by an *in situ* hybridization assay using a probe encompassing exons 46 to 51. ABCA12 mRNA was detected in the skin of wild-type animals by the antisense probe, but the same probe was unable to generate any signal of ABCA12 expression in animals homozygous for the targeted deletion (Fig. 1*D*). Consistent with the RNA analyses, immunoblots of proteins extracted from epidermis revealed no ABCA12 protein in null mice, but a band of the expected size was presented in heterozygotes and wild-type mice. All three groups of mice had similar levels of expression of the closely related ABCA1 transporter (Fig. 1*E*). In composite, these results indicate that deletion of exon 9 of *Abca12* prevents expression of ABCA12.

Abrogation of ABCA12 expression led to death in mice, as no homozygous null animals survived the immediate postnatal period. However, if day 18.5 embryos were genotyped, near Mendelian frequencies of each genotype were obtained (wt:het:null, 104:155:72). Larger genotyping studies will be needed to determine whether *Abca12*$^{-/-}$ animals have slightly reduced viability *in utero*, as suggested by the genotyping results, but the absence of the transporter is clearly compatible with embryonic development to term. After birth, if the null animals are kept in an ambient air environment, mortality is universal, indicating a vital role for ABCA12 in survival *ex utero*.

To investigate the cause of death of *Abca12*$^{-/-}$ mice, studies were carried out on late term E18.5 embryos delivered by cesarean section. When kept hydrated, the weight of *Abca12*$^{-/-}$ embryos was indistinguishable from that of wild-type and heterozygous littermates (wt, 0.96 $\pm$ 0.28 g, n = 16; heterozygous, 1.06 $\pm$ 0.26 g, n = 22; null 1.02 $\pm$ 0.21 g, n = 20; p = 0.44 wt *versus* null) (Fig. 2*A*). However, when exposed to ambient temperature and humidity, the *Abca12*$^{-/-}$ pups rapidly dehydrated within a matter of minutes, with their skin contracting and encasing them in a collodion-like shell (Fig. 2*B*). Consistent with a specific defect in skin function, histological analysis showed a markedly hyperkeratotic stratum corneum in the *Abca12*$^{-/-}$ mice (Fig. 2*C*). Further histological analysis did not reveal gross pathologies of the other major organs, including the lungs, which the Abca12$^{-/-}$ neonates were able to aerate, and which contain surfactant and type II pneumatocyte lamellar bodies as determined by electron microscopic analysis (supplemental Fig. S1).

Loss of the Interstitial Lamellar Barrier in the Abca12$^{-/-}$ *Skin Increases Trans-epidermal Water Loss*—The markedly thicken stratum corneum observed in the *Abca12*$^{-/-}$ animals and their rapid demise after birth suggested that the loss of ABCA12 activity had disrupted their epidermal permeability barrier. To test this hypothesis, E18.5 Abca12$^{-/-}$ embryos were stained with toluidine blue, a dye that does not penetrate the epidermis upon formation of the permeability barrier. As seen in Fig. 3*A*, the null mouse uniformly takes up the dye, whereas the wild-type littermate can effectively exclude it, consistent with the latter's ability to form an intact permeability barrier. To investigate the bi-directional function of the permeability

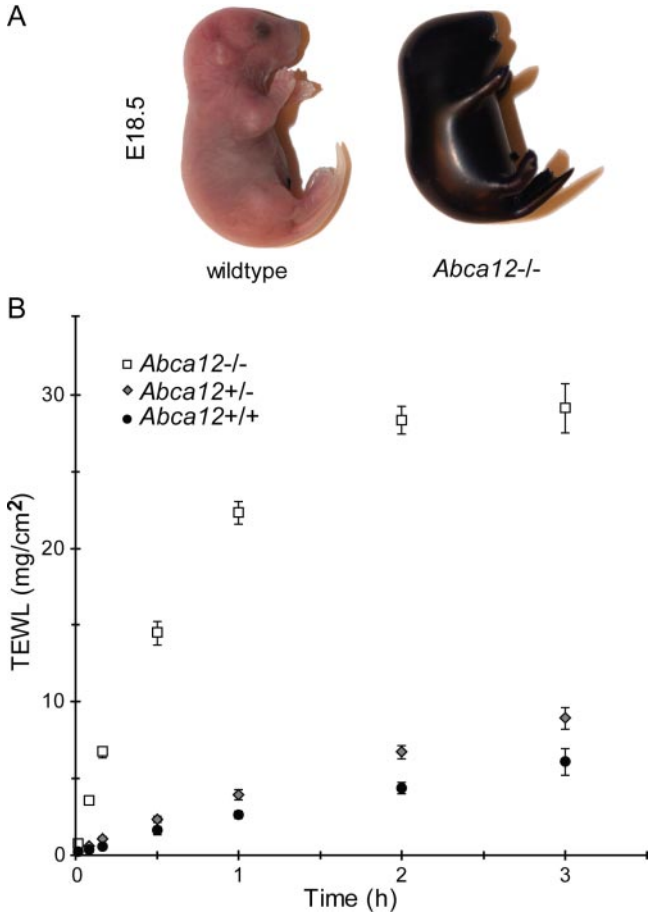

FIGURE 3. **Abca12$^{-/-}$ mice fail to develop the epidermal permeability barrier.** *A*, littermate E18.5 embryos stained with toluidine blue indicates loss of ABCA12 function increases inward permeability to this dye. *B*, loss of ABCA12 function significantly increases outward trans-epidermal water loss rates as measured in littermate E18.5 embryos using the gravimetric assay (*Abca12*$^{+/+}$, $n = 3$; *Abca12*$^{+/-}$, $n = 7$; *Abca12*$^{-/-}$, $n = 6$; ± S.E.: $p = 0.11$, *Abca12*$^{+/+}$ *versus Abca12*$^{+/-}$; $p = 0.00005$, *Abca12*$^{+/+}$ *versus Abca12*$^{-/-}$).

barrier, TEWL rates were measured. Skin samples from *Abca12*$^{+/+}$, *Abca12*$^{+/-}$, and *Abca12*$^{-/-}$ E18.5 embryos were tested for TEWL rates using a gravimetric assay. Confirming the results of the toluidine blue dye test, the TEWL assay demonstrated significantly greater water loss through the epidermis of *Abca12*$^{-/-}$ skin compared with that taken from wild-type or heterozygous mice (Fig. 3*B*). A slightly greater rate of water loss was noted from the heterozygous skin relative to the homozygous wild-type samples, but this trend did not reach statistical significance, consistent with the histological observations showing no gross abnormality of the skin of the E18.5 *Abca12*$^{+/-}$ embryos.

Having confirmed that loss of ABCA12 function had disrupted the epidermal permeability barrier, we then investigated the ultrastructural conformation of the epidermis that is known to be involved in the creation of the skin's barrier function. We were particularly interested in assessing whether the corneocytes of the thickened *Abca12*$^{-/-}$ stratum corneum lacked the characteristic interstitial lamellar lipid barrier, as has been reported in infants with the HI phenotype. As expected, *Abca12*$^{+/+}$ E18.5 embryos showed a clearly organized stratum corneum with interstitial lamellar material, as well as lamellar storage bodies in the stratum granulosum (Fig. 4, *A–D*). In contrast, their *Abca12*$^{-/-}$ littermates demonstrated a stratum corneum thickened ~6-fold that lacked organized lamellar structures in the interstitial spaces (Fig. 4, *E* and *F*). The interstitial spaces of the null skin were instead filled with a disorganized multivesicular material (Fig. 4*F*). Similarly, in the stratum granulosum of the *Abca12*$^{-/-}$ epidermis there was no evidence of intact lamellar storage bodies, although numerous multivesicular bodies were found, which are the presumed precursor of the lamellar body (Fig. 4, *G* and *H*). In aggregate, these findings demonstrate that loss of ABCA12 function in mice compromises the structural integrity of the skin's lamellar permeability barrier, leading to an inability to maintain water homeostasis, causing the demise of the newborn *Abca12*$^{-/-}$ pups after exposure to air.

Loss of ABCA12 Function Does Not Alter E18.5 Epidermal Proliferation Indices but Is Associated with Altered Keratin 14 Expression, Filaggrin Solubility, and Parakeratosis—To further explore the cause of the thickened stratum corneum of *Abca12*$^{-/-}$ skin, we investigated whether loss of ABCA12 function induced aberrant cellular proliferation of the epidermis. Epidermal DNA synthesis of E18.5 embryos *in utero* was measured after injecting bromodeoxyuridine (BrdUrd) into the peritoneum of the pups' mother. After 1 h of exposure, embryos were sacrificed, and epidermal nuclei positive for BrdUrd were detected in skin sections using an anti-BrdUrd antibody. As shown in Fig. 5*A*, BrdUrd-positive cells were observed in the basal layers of both *Abca12*$^{+/+}$ and *Abca12*$^{-/-}$, but increased numbers of BrdUrd-positive cells were not found in the *Abca12*$^{-/-}$ basal layer, nor in the normally quiescent upper cellular layers of the stratum spinosum and stratum granulosum (supplemental Fig. S2). We considered whether the thicken stratum corneum and/or loss of ABCA12 transport activity may have inhibited access of BrdUrd to the proliferating cellular layers of the *Abca12*$^{-/-}$ epidermis, thus giving an underestimate of cell division. To address this possibility, we assessed cellular proliferation by an alternative method, directly staining for the proliferation marker Ki67. Consistent with the BrdUrd incorporation assay, expression of Ki67 in *Abca12*$^{-/-}$ epidermis was not found to be increased over that seen in littermate paired *Abca12*$^{+/+}$ samples (Fig. 5*B*). Finally, we stained for Keratin 6, which is expressed in epidermal keratinocytes that hyperproliferate, but no Keratin 6 staining was observed in the cellular layers of the *Abca12*$^{-/-}$ epidermis (data not shown). Considered together, our evidence in late term *Abca12*$^{-/-}$ embryos provided no evidence that aberrant cellular proliferation rates were driving the expansion of the stratum corneum.

Because an increase in proliferation markers was not observed in the *Abca12*$^{-/-}$ epidermis, we explored whether loss of ABCA12 had altered the expression of the keratins and cornified envelope proteins that are associated with the differentiation and maturation of basal cells into granulocytes and corneocytes. Keratin 14 expression, a marker of the basal layer, was detected in the *Abca12*$^{+/+}$ skin only in the lowest cellular layer of the epidermis. Interestingly, in the *Abca12*$^{-/-}$ epidermis, K14 expression was more expansive and appeared to persist in first cells of the stratum spinosum (Fig. 5*C*). Expression of

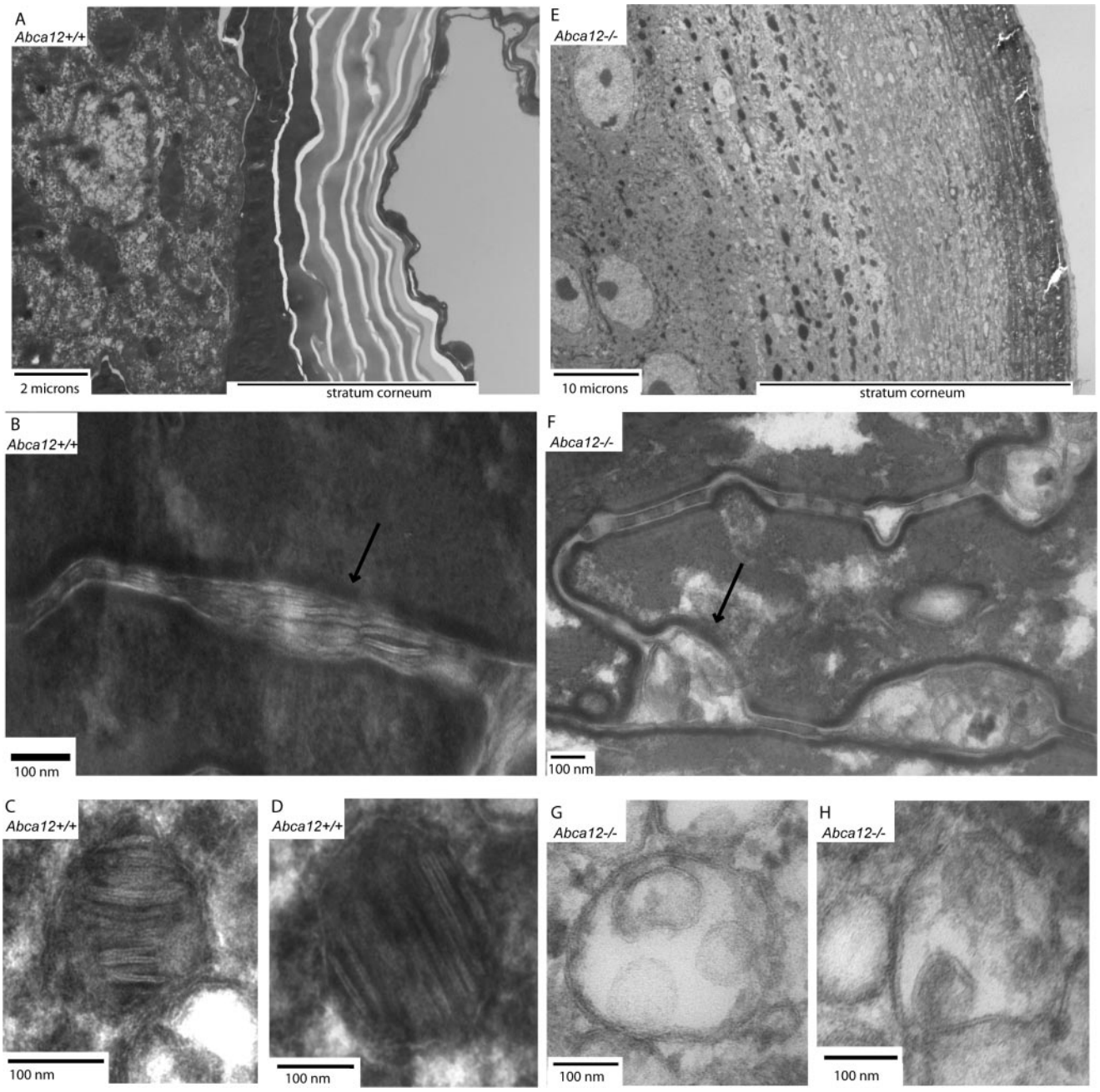

FIGURE 4. **Loss of ABCA12 transport function induces hyperkeratosis of the stratum corneum (*SC*) and disrupts interstitial lamellar lipid structure.** *A*, electron micrograph of the *Abca12*$^{+/+}$ epidermis showing a normal SC (10,000×). *E*, *Abca12*$^{-/-}$ epidermis showing massive hyperkeratosis of the SC (2000× magnification, which was required to capture the expanded SC). *B*, interstitial spaces of the *Abca12*$^{+/+}$ SC demonstrate the lipid lamellar structures required for permeability barrier function (arrow, 80,000×), which are absent and replaced by a disorganized multivesicular material in the interstitial spaces of the *Abca12*$^{-/-}$ SC (*F*, *arrow*, 80,000×). *C* and *D*, lamellar storage bodies present in the *Abca12*$^{+/+}$ stratum granulosum (*C* and *D*, 150,000×). The *Abca12*$^{-/-}$ stratum granulosum lacked lamellar storage bodies but did contain numerous multivesicular bodies, the presumptive precursor of the lamellar body (*G* and *H*, 150,000×).

Keratin 10, which marks cells in the suprabasal layers that have initiated terminal differentiation, was detected in the spinosum and granular layers and was found to be similar between the wild-type and null samples (Fig. 5*D*). The late differentiation markers loricrin and filaggrin, which are expressed by granulocytes and are incorporated into the cornified envelope, were present in the *Abca12*$^{-/-}$ granular and stratum corneum layers. Compared with the staining of these same proteins in wild-type skin, however, the distribution appeared more punctate, particularly for filaggrin (Fig. 5, *E* and *F*). Because skin from HI patients has been associated with a block in the processing of profilaggrin to filaggrin (20), immunoblots were used to measure amounts of these products that were extractable with either a mild detergent or with the strong denaturant, urea. Significantly, less processed filaggrin was detected in the detergent extracts of *Abca12*$^{-/-}$ samples, whereas profilaggrin, K14, involucrin, and β-actin levels were similar (Fig. 6*A*). In contrast, both profilaggrin and filaggrin levels were as high, if not higher, in the null samples extracted with a strong denaturant (Fig. 6*B*). These results suggest that loss of ABCA12 does not induce a

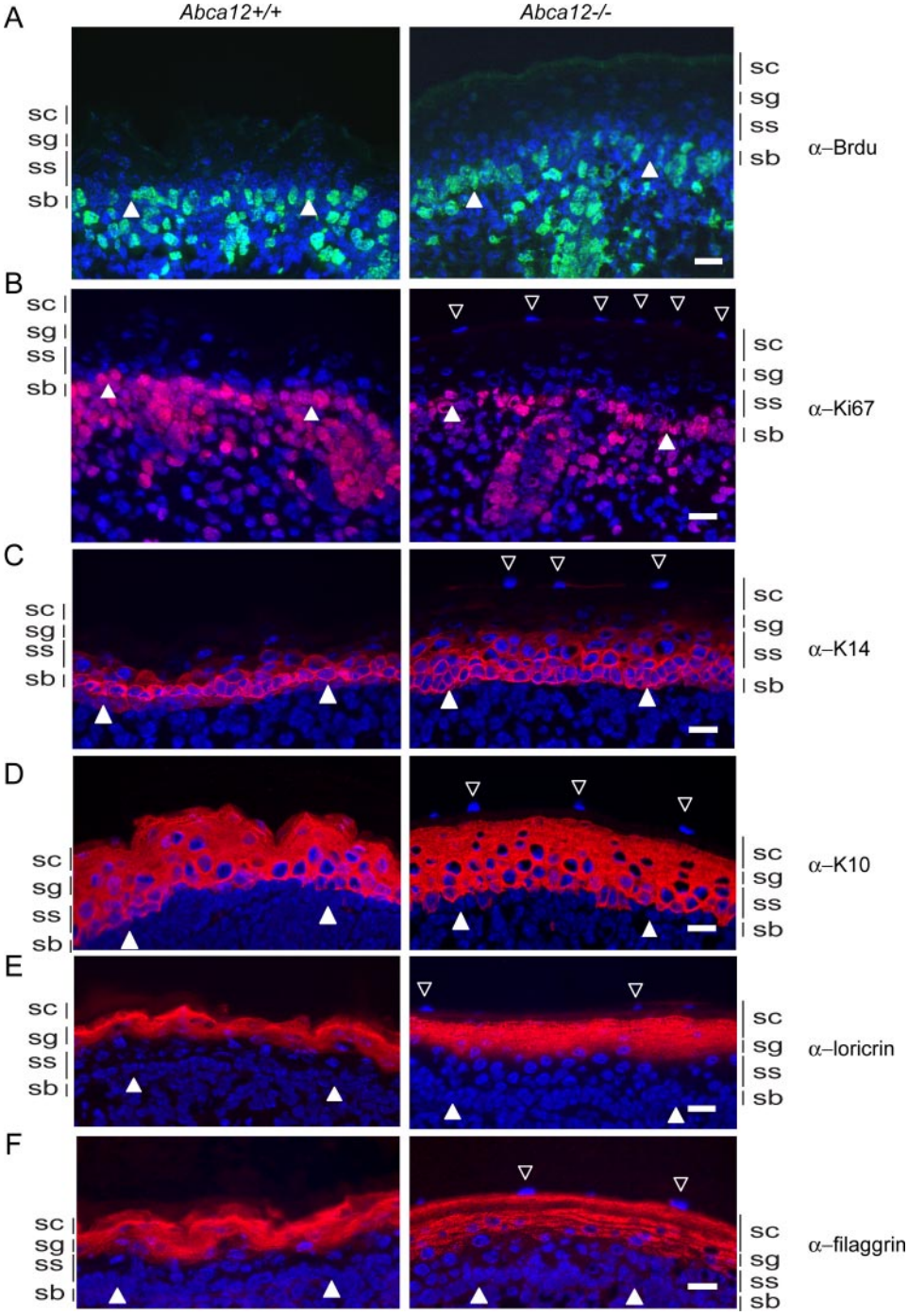

FIGURE 5. **Loss of ABCA12 function does not alter E18.5 epidermal cell proliferation indices.** *A*, DNA synthesis rates are similar in E18.5 *Abca12*$^{+/+}$ and *Abca12*$^{-/-}$ embryos as determined by *in utero* incorporation of the thymidine analogue, BrdUrd. Shown are skin sections from littermate-paired embryos labeled for 1 h and stained with an anti-BrdUrd antibody (*green*) and counterstained for nuclei with Hoechst 33258 (*blue*). *B*, staining for the Ki67 proliferation maker (*magenta*) is also similar in wild-type and null samples and is confined to the basal layer. *C*, staining for the basal cell differentiation marker Keratin 14 (*red*) is expanded into the first cell layer of the stratum spinosum in the *Abca12*$^{-/-}$ epidermis. *D*, staining for Keratin 10 is similar between the genotypes and is largely confined to the stratum spinosum and stratum granulosum. Staining for the cornified envelope marker loricrin (*E*) and filaggrin (*F*) show a more granular distribution in the *Abca12*$^{-/-}$ epidermis. The basal epidermal layer is indicated by *filled arrowheads*, and *open arrowheads* denote parakeratotic nuclei in the *Abca12*$^{-/-}$ stratum corneum. *Scale bar*, 20 μm.

block in the processing of profilaggrin to filaggrin, although the solubility characteristics of the protein are altered. Finally, it was noted that the *Abca12*$^{-/-}$ epidermis exhibited signs of abnormal parakeratosis, because the uppermost layers of the stratum corneum were found consistently to stain positively for nuclear material (*open triangles* denote stained nuclei in the stratum corneum, Fig. 5). Thus, in mice, loss of ABCA12 function does not block filaggrin processing, but it does affect the extraction properties of that protein from skin, and is associated with a persistence of nuclear material in the stratum corneum.

Lipid Mass Spectrometry Profiling of Abca12$^{-/-}$ *Skin Shows Loss of Cer(EOS) and Accumulation of GlucosylCer(EOS)*—The ultrastructural analysis described above indicated that ABCA12 function was critical for maintaining the characteristic lamellar appearance of the interstitial spaces in the stratum corneum. To form these structures of the permeability barrier, a complex mix of lipids are packaged into lamellar storage bodies and subsequently extruded into the extracellular space of the stratum corneum. This mix of lipids includes cholesterol, free fatty acids, phospholipids, and ceramides. Ceramide composition and structure are particularly important for the formation of the permeability barrier and its lamellar structure. The very hydrophobic linoleic esters of ω-hydroxy long-chain ceramides are thought to have unique biophysical characteristics that aid in formation of the lamellar barrier. To gain further insight into ABCA12 function, keeping in mind its membership in a lipid transporter family, we sought to characterize the level of the various lipids that form the lamellar barrier, using a broad mass spectrometry approach. Total cholesterol levels in the skin of the Abca12$^{-/-}$ mice did not differ significantly from that of littermate matched *Abca12*$^{+/+}$ mice (supplemental Fig. S3). This was also the case for total phosphatidylcholine, phosphatidylethanolamine, phosphatidylserine, sphingomyelin, and free fatty acids (Table 1 and supplemental Figs. S4–S8). However, total ceramide levels were significantly reduced in the skin of *Abca12*$^{-/-}$ mice (Table 1), and this reduction was most profound for levels of the linoleic esters of ω-hydroxy long-chain ceramides (Fig. 7,

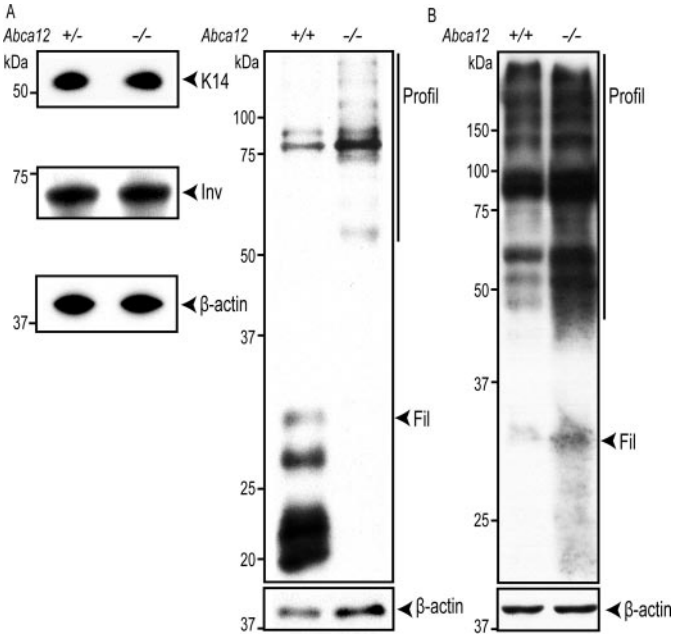

FIGURE 6. **Loss of ABCA12 function alters filaggrin solubility but not processing.** *A*, immunoblot analysis of Keratin 14 (*K14*), involucrin (*Inv*), profilaggrin (*Profil*), and filaggrin (*Fil*) extracted from the E18.5 skin using mild detergent buffer. *B*, profilaggrin and filaggrin extracted from skin using denaturing buffer.

TABLE 1
Loss of ABCA12 function significantly reduces skin ceramide levels

Lipid	ABCA12$^{+/+}$	ABCA12$^{-/-}$	*p* value[a]
Ceramide[b]	0.67 ± 0.28	0.35 ± 0.17	0.04
Phosphatidylcholine	3.98 ± 1.02	3.34 ± 0.41	0.23
Phosphatidylethanolamine	1.31 ± 0.62	1.09 ± 0.14	0.46
Phosphatidylinositol	0.29 ± 0.08	0.26 ± 0.05	0.38
Phosphatidylserine	0.10 ± 0.03	0.07 ± 0.01	0.08
Sphingomyelin	0.74 ± 0.21	0.66 ± 0.08	0.43
Cholesterol[c]	1.74 ± 0.15	1.68 ± 0.15	0.51
Free fatty acid	16.2 ± 3.6	20.4 ± 0.5	0.27

[a] *p* values are derived from a two-tailed Student's *t*-test ($n = 5$, ±S.E.).
[b] Ceramide, phospholipid, and free fatty acid values are expressed as nanomoles/mg of skin.
[c] Cholesterol values are expressed as micrograms/mg of skin tissue.

A and *B*). Because these ceramides are formed from glucosylceramide precursors (32), which are the substrates packaged into the lamellar storage bodies in the epidermal granular layer (33), we further analyzed levels of glucosyl Cer(EOS) precursors. As opposed to the 90% drop in the levels of the Cer(EOS) species, the corresponding glucosylCer(EOS) species were increased by nearly 5-fold when ABCA12 function was lost (Fig. 7*B*). The Cer(EOS) and GlcCer(EOS) were identified by scanning for the sphingoid base. To confirm their identities, product ion analysis was performed. Collision-induced fragmentation in negative mode of the $[M + OAc]^-$ ions for each of the long-chain ceramides shown in Fig. 7 (and for the most prominent GlcCers (d18:1/50:2 and d18:1/52:3)), produced an *m*/*z* 279 fragment. This mass is consistent with a 18:2 anion, as expected for a linoleic ester of the ω-hydroxy ceramide. Loss of ABCA12 also affected the levels of un-esterifed Cer(OS) species, but this effect was not as profound and varied relative to the acyl chain length (supplemental Fig. S9). The Cer(NS) and GlcCer(NS) species were largely unaffected by loss of ABCA12 (supplemental Figs. S9 and S10). Thus, a broad profiling of lipids indicates ABCA12 transport function is critical for maintaining skin linoleic esters of ω-hydroxy long-chain ceramides and when this function is lost, glucosyl precursors of these ceramides accumulate.

DISCUSSION

In this study, we have explored the function of ABCA12 by investigating homologous recombinant mice lacking its expression. *Abca12*$^{-/-}$ mice developed to embryonic day 18.5 with near Mendelian frequencies, but universally failed to survive *ex utero*. The skin of these mice has a markedly expanded stratum corneum composed of disorganized and poorly condensed corneocytes that lack their characteristic interstitial lipid lamellae. The loss of this lipid lamellae results in formation of a defective water permeability barrier in the skin, leading to massive water loss from the *Abca12*$^{-/-}$ epidermis. A broad-scale lipidomic analysis of *Abca12*$^{-/-}$ skin detected a reduction in the levels of linoleic esters of ω-hydroxy long-chain ceramides that was associated with a corresponding increase in the glucosylated precursors of those same lipids. These data indicate that ABCA12 plays an essential role in the formation of the skin's permeability barrier via effects on a ceramide that plays a specialized role in generating that barrier.

In children and adults, mutations in ABCA12 have been associated with disruption of the lamellar permeability barrier and skin ichthyoses of variable severity. Initially, in 2003, ABCA12 missense mutations were associated with lamellar ichthyosis type 2, a less severe non-fatal scaling condition of the skin (6). Subsequently, in 2005, two reports associated truncation and deletion mutations in ABCA12 with the more severe and often fatal harlequin ichthyosis (3, 5). The HI phenotype is characterized by a markedly thickened stratum corneum and loss of interstitial lamellar structures between the corneocytes of the expanded stratum corneum. The skin of the *Abca12*$^{-/-}$ mice analyzed here recapitulated these features of HI. As estimated by our electron micrographs, the *Abca12*$^{-/-}$ stratum corneum is expanded 5- to 6-fold, and the corneocytes within this expanded SC lacked all evidence of interstitial lamellar structures. Consistent with a loss of corneocyte interstitial lamellae, the granulocyte layer of the *Abca12*$^{-/-}$ epidermis showed no evidence of the lamellar storage organelles that are the presumptive source of the lipids that form the corneocyte interstitial lamellae. However, we did observe numerous multivesicular bodies in the *Abca12*$^{-/-}$granulocytes, which may represent lamellar bodies precursors that are the source of the disorganized multivesicular material observed in the interstitial spaces of the expanded *Abca12*$^{-/-}$stratum corneum. These ultrastructural observations are entirely consistent with the functional assays we performed that indicated a permeability barrier failure, *i.e.* rapid dehydration of the null animals, increased skin water loss by gravimetric assay, and an inability to exclude the water soluble toluidine blue dye.

During the preparation of this report, Yanagi *et al.* (34) published on-line an independent investigation of their own *Abca12*$^{-/-}$ mice. Although the skin histological and ultrastructural findings in their mice are similar to those we report, there are several interesting differences in the two studies. Yanagi *et al.* concluded that their *Abca12*$^{-/-}$ mice failed to inflate their lungs due to a deficiency in pulmonary surfactant and likely

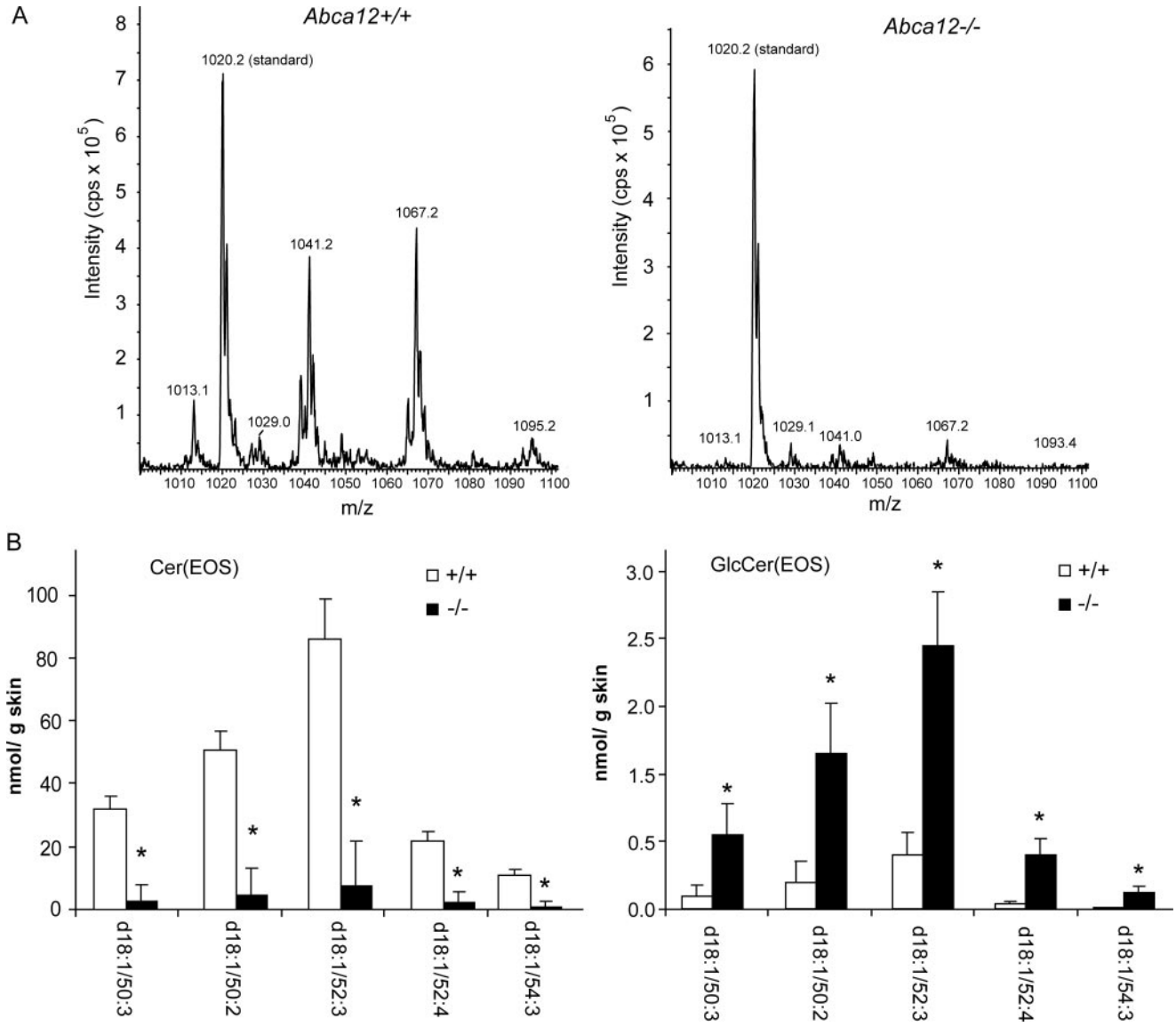

FIGURE 7. **Loss of ABCA12 transport function blocks Cer(EOS) formation and induces a buildup of GlcCer(EOS).** *A*, representative spectra showing the loss of the Cer(EOS) peaks in the *Abca12*$^{-/-}$ skin sample (peak at 1020.2 *m/z* derived from the standard mixture is shown for comparison). *B*, quantitation of the Cer(EOS) and corresponding glucosyl Cer(EOS) species in the wild-type and null skin samples ($n = 5$, ± S.E.; *, $p < 0.05$).

died from respiratory failure. We did not find this to be the case in the mice we produced, because they were able to expand and aerate their lungs, as evidenced by histological exam and the ability of *Abca12*$^{-/-}$ lungs to float in phosphate-buffered saline (supplemental Fig. S1, *A* and *B*). Furthermore, electron micrographs of *Abca12*$^{-/-}$ lungs showed type II alveolar cells that were able to form lamellar bodies, unlike the epidermal cells in these animals, and secrete surfactant in a normal manner (supplemental Fig. S1*C*). Finally, when we kept *Abca12*$^{-/-}$ mice in a highly hydrated environment, they could survive and breathe for several hours after birth, a finding inconsistent with an inability to aerate the lung due to the lack of surfactant production (supplemental video). Mice that were not hydrated died much more rapidly.

Further studies will be needed to reconcile these disparate observations, because they could reflect differences in the genetic disruptions engineered into the mice or some strain variability. Although we have found no evidence for expression of full-length ABCA12 protein in our null mice using either a C-terminal antibody (Fig. 1*E*) or an N-terminal antibody (data not shown), we cannot exclude the possibility that a truncated transcript derived from the rearranged locus in the mice could lead to some functional activity that accounts for the differences in lung phenotype seen. Although we cannot rule out a role for ABCA12 in the lung, several observations make us cautious about accepting a major role for ABCA12 in pulmonary function. Previously, we reported the generation of mice lacking ABCA3, and those animals died much more rapidly after birth than did Abca12$^{-/-}$ mice (16). The Abca3$^{-/-}$ mice were never able to inflate their lungs, a finding subsequently confirmed by several other groups, and they failed to form lung lamellar bodies and secrete surfactant into the alveolar space (15, 16, 35, 36). Furthermore, we found ABCA3 to be highly expressed in the lung, whereas ABCA12 is not (Ref. 16 and data not shown). Finally, our reading of the literature does not suggest that immediate respiratory compromise is a common fea-

ture of human harlequin ichthyosis, whereas children lacking ABCA3 activity cannot breathe without assistance. For all of these reasons, we believe that ABCA3 is the major surfactant transporter in the lung, whereas ABCA12's primary locus of activity is the skin.

To gain insight into the primary function of ABCA12, we hypothesized that it would play a role in lipid transport and therefore influence lipid levels in the skin. To explore that hypothesis, gas chromatography and electrospray ionization mass spectrometry approaches were used to profile a broad spectrum of skin lipids. Previously, we used this approach to show a unique and specific role for ABCA3 in maintaining lung levels of phosphatidylglycerol and short-chain phosphatidylcholine species, which are packaged in lamellar surfactant storage organelles in the type II alveolar cells (16). In the current study, we found that loss of ABCA12 transport function causes a >90% reduction in the amount of linoleic esters of long-chain ω-hydroxyceramides. Associated with this finding was an ~5-fold increase in the levels of the glucosyl precursors of these ω-hydroxyceramide esters. As studies in β-glucocerebrosidase-deficient fibroblasts have shown that cells can prevent significant glucosylceramide accumulation by metabolizing these lipids to other sphingolipid forms, it is perhaps not surprising that the decline in ceramide mass we measured was not matched by an equivalent mass increase in glucosylceramides (37).

The quantitative and specific molecular characterization of lipid species affected by the loss of ABCA12 that we report in this study are consistent with the qualitative, immunohistochemical results reported by Yanagi *et al.* (34), who noted a loss of ceramide staining in the stratum corneum of their mice, as well as accumulation of glucosylceramide staining intracellularly. Because glucosylceramides are packaged in the lamellar bodies of skin granulocytes and subsequently converted by β-glucocerebrosidase to the corresponding non-glycated ceramides (38), it is tempting to speculate that ABCA12 does indeed play a direct role in lipid transport involving these specialized ceramides. Loss of this transport activity would thereby result in the failure to extrude these glucosylated precursors into the extracellular environment, where β-glucocerebrosidase processes them.

Whereas more direct experimental data are needed to establish the mechanism proposed above, several lines of evidence support this hypothesis. As sphingomyelin and ceramide are produced in the same biosynthetic pathway, but sphingomyelin levels were unaffected by the loss of ABCA12 activity, our data indicate that ABCA12 is not essential for generalized sphingolipid synthesis. Similarly, we found that loss of ABCA12 activity did not significantly affect skin-free fatty acids levels, including that of linoleic acid, which indicates that the loss of the linoleic ceramide esters was not secondary to insufficient cellular linoleate supplies. Although it is formally possible that ABCA12 could play a role in transporting β-glucocerebrosidase rather than its substrate lipids, studies in animals either lacking the enzyme in the skin or treated with an enzyme inhibitor have reported no disruption of the epidermal lamellar body structure (38, 39). Additionally, loss of β-glucocerebrosidase, or its activator Saposin-C caused a different spectrum of ceramide and glucosylceramide alterations in the skin than those we report here in the Abca12$^{-/-}$ mice (40, 41). Thus, we believe that current data are most consistent with a model that posits ABCA12 functions as a lipid transporter that is required for the transport of a specialized class of ceramides into the lamellar body.

Our findings with ABCA12, in concert with studies of the other ABCA family members, suggest a general paradigm for the biological role of members of the ABCA transporter family. This paradigm posits that each member of the ABCA family will have a unique lipid substrate or spectrum of substrates that it transports across a cellular membrane. This transport enables the lipid to associate with an acceptor protein or enzyme that resides on the distal side of the membrane that must be crossed. We further suggest that each member of the transporter family has evolved to enable transport of a specialized class of lipids and that the expression of the transporter may be restricted in a cell or tissue-specific fashion to enable a specialized function. Supporting the latter hypothesis in the current study are our findings that several classes of skin lipid levels shown to be substrates for transport by other members of the ABCA family were unaffected by the loss of ABCA12 (16).

How the loss of ABCA12 transport function provokes the development of an extremely hyperkeratotic stratum corneum is unclear. It had been proposed that in response to the loss of the permeability barrier, the epidermis mounts a compensatory cellular proliferation response in an effort to restore the barrier (42). As analyzed by BrdUrd incorporation into epidermal keratinocytes and by expression of independent proliferation markers in these cells, we found no evidence that loss of ABCA12 levels induced cellular proliferation in the epidermis. However, we did find evidence of altered K14 expression in the basal layer, and of residual nuclear material in the thickened stratum corneum. Additionally, the solubility of filaggrin in tissue extracts was affected by loss of ABCA12 expression. How these changes relate to a loss of ABCA12 function is unclear, but they may be secondary to signals generated by the loss of the skin ceramide barrier. The generation of ABCA12 null mice should facilitate future investigations into these unanswered questions.

In summary, our results indicate that ABCA12 plays a critical role in the formation of the skin's permeability barrier via an effect on the generation of a highly specialized class of ceramide esters. These findings raise the possibility that strategies designed to increase the amount of these specific ceramides in the skin could ameliorate defects in skin function in individuals with harlequin ichthyosis and, potentially, other disorders of the skin lipid permeability barrier.

Acknowledgments—We thank Dr. Dennis Brown (Program in Membrane Biology) for electron microscopy support and Mary Roth for mass spectrometry support.

REFERENCES

1. Akiyama, M. (2006) *J. Dermatol. Sci.* **42,** 83–89
2. Akiyama, M., Sakai, K., Hatamochi, A., Yamazaki, S., McMillan, J. R., and Shimizu, H. (2008) *Br. J. Dermatol.* **158,** 864–867
3. Akiyama, M., Sugiyama-Nakagiri, Y., Sakai, K., McMillan, J. R., Goto, M., Arita, K., Tsuji-Abe, Y., Tabata, N., Matsuoka, K., Sasaki, R., Sawamura, D.,

and Shimizu, H. (2005) *J. Clin. Invest.* **115,** 1777–1784
4. Annilo, T., Shulenin, S., Chen, Z. Q., Arnould, I., Prades, C., Lemoine, C., Maintoux-Larois, C., Devaud, C., Dean, M., Denefle, P., and Rosier, M. (2002) *Cytogenet. Genome Res.* **98,** 169–176
5. Kelsell, D. P., Norgett, E. E., Unsworth, H., Teh, M. T., Cullup, T., Mein, C. A., Dopping-Hepenstal, P. J., Dale, B. A., Tadini, G., Fleckman, P., Stephens, K. G., Sybert, V. P., Mallory, S. B., North, B. V., Witt, D. R., Sprecher, E., Taylor, A. E., Ilchyshyn, A., Kennedy, C. T., Goodyear, H., Moss, C., Paige, D., Harper, J. I., Young, B. D., Leigh, I. M., Eady, R. A., and O'Toole, E. A. (2005) *Am. J. Hum. Genet.* **76,** 794–803
6. Lefevre, C., Audebert, S., Jobard, F., Bouadjar, B., Lakhdar, H., Boughdene-Stambouli, O., Blanchet-Bardon, C., Heilig, R., Foglio, M., Weissenbach, J., Lathrop, M., Prud'homme, J. F., and Fischer, J. (2003) *Hum. Mol. Genet.* **12,** 2369–2378
7. Rajpar, S. F., Cullup, T., Kelsell, D. P., and Moss, C. (2006) *Br. J. Dermatol.* **155,** 204–206
8. Bodzioch, M., Orso, E., Klucken, J., Langmann, T., Bottcher, A., Diederich, W., Drobnik, W., Barlage, S., Buchler, C., Porsch-Ozcurumez, M., Kaminski, W. E., Hahmann, H. W., Oette, K., Rothe, G., Aslanidis, C., Lackner, K. J., and Schmitz, G. (1999) *Nat. Genet.* **22,** 347–351
9. Brooks-Wilson, A., Marcil, M., Clee, S. M., Zhang, L. H., Roomp, K., van Dam, M., Yu, L., Brewer, C., Collins, J. A., Molhuizen, H. O., Loubser, O., Ouelette, B. F., Fichter, K., Ashbourne-Excoffon, K. J., Sensen, C. W., Scherer, S., Mott, S., Denis, M., Martindale, D., Frohlich, J., Morgan, K., Koop, B., Pimstone, S., Kastelein, J. J., and Hayden, M. R. (1999) *Nat. Genet.* **22,** 336–345
10. Lawn, R. M., Wade, D. P., Garvin, M. R., Wang, X., Schwartz, K., Porter, J. G., Seilhamer, J. J., Vaughan, A. M., and Oram, J. F. (1999) *J. Clin. Invest.* **104,** R25–R31
11. Rust, S., Rosier, M., Funke, H., Real, J., Amoura, Z., Piette, J. C., Deleuze, J. F., Brewer, H. B., Duverger, N., Denefle, P., and Assmann, G. (1999) *Nat. Genet.* **22,** 352–355
12. Brasch, F., Schimanski, S., Muhlfeld, C., Barlage, S., Langmann, T., Aslanidis, C., Boettcher, A., Dada, A., Schroten, H., Mildenberger, E., Prueter, E., Ballmann, M., Ochs, M., Johnen, G., Griese, M., and Schmitz, G. (2006) *Am. J. Respir. Crit. Care Med.* **174,** 571–580
13. Bullard, J. E., Wert, S. E., Whitsett, J. A., Dean, M., and Nogee, L. M. (2005) *Am. J. Respir. Crit. Care Med.* **172,** 1026–1031
14. Shulenin, S., Nogee, L. M., Annilo, T., Wert, S. E., Whitsett, J. A., and Dean, M. (2004) *N. Engl. J. Med.* **350,** 1296–1303
15. Cheong, N., Zhang, H., Madesh, M., Zhao, M., Yu, K., Dodia, C., Fisher, A. B., Savani, R. C., and Shuman, H. (2007) *J. Biol. Chem.* **282,** 23811–23817
16. Fitzgerald, M. L., Xavier, R., Haley, K. J., Welti, R., Goss, J. L., Brown, C. E., Zhuang, D. Z., Bell, S. A., Lu, N., McKee, M., Seed, B., and Freeman, M. W. (2007) *J. Lipid Res.* **48,** 621–632
17. Allikmets, R., Shroyer, N. F., Singh, N., Seddon, J. M., Lewis, R. A., Bernstein, P. S., Peiffer, A., Zabriskie, N. A., Li, Y., Hutchinson, A., Dean, M., Lupski, J. R., and Leppert, M. (1997) *Science* **277,** 1805–1807
18. Allikmets, R., Singh, N., Sun, H., Shroyer, N. F., Hutchinson, A., Chidambaram, A., Gerrard, B., Baird, L., Stauffer, D., Peiffer, A., Rattner, A., Smallwood, P., Li, Y., Anderson, K. L., Lewis, R. A., Nathans, J., Leppert, M., Dean, M., and Lupski, J. R. (1997) *Nat. Genet.* **15,** 236–246
19. Weng, J., Mata, N. L., Azarian, S. M., Tzekov, R. T., Birch, D. G., and Travis, G. H. (1999) *Cell* **98,** 13–23
20. Dale, B. A., Holbrook, K. A., Fleckman, P., Kimball, J. R., Brumbaugh, S., and Sybert, V. P. (1990) *J. Invest. Dermatol.* **94,** 6–18
21. Milner, M. E., O'Guin, W. M., Holbrook, K. A., and Dale, B. A. (1992) *J. Invest. Dermatol.* **99,** 824–829
22. Kim, W. S., Fitzgerald, M. L., Kang, K., Okuhira, K., Bell, S. A., Manning, J. J., Koehn, S. L., Lu, N., Moore, K. J., and Freeman, M. W. (2005) *J. Biol. Chem.* **280,** 3989–3995
23. Fitzgerald, M. L., Mendez, A. J., Moore, K. J., Andersson, L. P., Panjeton, H. A., and Freeman, M. W. (2001) *J. Biol. Chem.* **276,** 15137–15145
24. Epp, N., Furstenberger, G., Muller, K., de Juanes, S., Leitges, M., Hausser, I., Thieme, F., Liebisch, G., Schmitz, G., and Krieg, P. (2007) *J. Cell Biol.* **177,** 173–182
25. Resing, K. A., Walsh, K. A., and Dale, B. A. (1984) *J. Cell Biol.* **99,** 1372–1378
26. Weiner, L., Han, R., Scicchitano, B. M., Li, J., Hasegawa, K., Grossi, M., Lee, D., and Brissette, J. L. (2007) *Cell* **130,** 932–942
27. Hou, S. Y., Mitra, A. K., White, S. H., Menon, G. K., Ghadially, R., and Elias, P. M. (1991) *J. Invest. Dermatol.* **96,** 215–223
28. Horsley, V., O'Carroll, D., Tooze, R., Ohinata, Y., Saitou, M., Obukhanych, T., Nussenzweig, M., Tarakhovsky, A., and Fuchs, E. (2006) *Cell* **126,** 597–609
29. Hardman, M. J., Sisi, P., Banbury, D. N., and Byrne, C. (1998) *Development* **125,** 1541–1552
30. Ting, S. B., Caddy, J., Hislop, N., Wilanowski, T., Auden, A., Zhao, L. L., Ellis, S., Kaur, P., Uchida, Y., Holleran, W. M., Elias, P. M., Cunningham, J. M., and Jane, S. M. (2005) *Science* **308,** 411–413
31. Moore, K. J., Kunjathoor, V. V., Koehn, S. L., Manning, J. J., Tseng, A. A., Silver, J. M., McKee, M., and Freeman, M. W. (2005) *J. Clin. Invest.* **115,** 2192–2201
32. Jennemann, R., Sandhoff, R., Langbein, L., Kaden, S., Rothermel, U., Gallala, H., Sandhoff, K., Wiegandt, H., and Grone, H. J. (2007) *J. Biol. Chem.* **282,** 3083–3094
33. Freinkel, R. K., and Traczyk, T. N. (1985) *J. Invest. Dermatol.* **85,** 295–298
34. Yanagi, T., Akiyama, M., Nishihara, H., Sakai, K., Nishie, W., Tanaka, S., and Shimizu, H. (2008) *Hum. Mol. Genet.* **17,** 3075–3083
35. Ban, N., Matsumura, Y., Sakai, H., Takanezawa, Y., Sasaki, M., Arai, H., and Inagaki, N. (2007) *J. Biol. Chem.* **282,** 9628–9634
36. Hammel, M., Michel, G., Hoefer, C., Klaften, M., Muller-Hocker, J., de Angelis, M. H., and Holzinger, A. (2007) *Biochem. Biophys. Res. Commun.* **359,** 947–951
37. Saito, M., and Rosenberg, A. (1985) *J. Biol. Chem.* **260,** 2295–2300
38. Holleran, W. M., Ginns, E. I., Menon, G. K., Grundmann, J. U., Fartasch, M., McKinney, C. E., Elias, P. M., and Sidransky, E. (1994) *J. Clin. Invest.* **93,** 1756–1764
39. Holleran, W. M., Takagi, Y., Menon, G. K., Legler, G., Feingold, K. R., and Elias, P. M. (1993) *J. Clin. Invest.* **91,** 1656–1664
40. Doering, T., Holleran, W. M., Potratz, A., Vielhaber, G., Elias, P. M., Suzuki, K., and Sandhoff, K. (1999) *J. Biol. Chem.* **274,** 11038–11045
41. Doering, T., Proia, R. L., and Sandhoff, K. (1999) *FEBS Lett.* **447,** 167–170
42. Elias, P. M., Williams, M. L., Holleran, W. M., Jiang, Y. J., and Schmuth, M. (2008) *J. Lipid Res.* **49,** 697–714